

SEMI-EMPIRICAL CHARACTERIZATION OF FLOATING-RING BEARING FOR IMPROVED HIGH-SPEED TURBOMACHINERY PERFORMANCE

Tamunodukobipi Daniel¹, Tamunodukobipi Godgift Daniel², Igoma³, Emughiphel Nelson⁴, Yong-Bok Lee⁵

¹Marine Engineering Department, Faculty of Engineering, Rivers State University, Port Harcourt, Nigeria.

²Marine Engineering Department, Faculty of Engineering, Nigeria Maritime University, Okerenkoko, Delta State, Nigeria.

³Sustainable Energy Research Division, Korea Institute of Science and Technology (KIST), Seoul, South Korea

DOI: <https://www.doi.org/10.58257/IJPREMS39309>

ABSTRACT

Floating-ring bearings (FRBs) play a crucial role in high-speed turbomachinery by providing improved rotordynamic stability and load-bearing capacity. This study presents a semi-empirical characterization of FRB performance, focusing on the relationships between ring eccentricity, speed ratio, and force coefficients. Results indicate that the ring's eccentricity (ϵ_2) is strongly influenced by the journal eccentricity (ϵ_1) in low clearance ratios (c_2/c_1), but this dependence weakens as c_2/c_1 increases. The ring-to-journal speed ratio (NR/NJ) is primarily governed by the inner-film Sommerfeld number (Sn_1), exhibiting a sharp decline with increasing Sn_1 due to variations in rotor speed and bearing load. The evaluation of FRB force coefficients reveals that direct stiffness components (K_{xx} , K_{yy}) vary non-monotonically with Sn_1 , while cross-coupled stiffness terms (K_{xy} , K_{yx}) become significant at near-centre operations, posing potential instability risks. The direct damping coefficients (C_{xx} , C_{yy}) demonstrate high sensitivity to Sn_1 and ϵ_1 , with C_{yy} exhibiting particularly strong damping effects in light-load, high-speed conditions, thereby enhancing overall stability. These findings provide valuable insights for optimizing FRB design and operation in turbomachinery, ensuring improved rotordynamic performance, stability, and efficiency.

Keywords: Bearing Instability, Dynamic Characteristics of Bearings, Floating-ring Bearings Characterisation, High-speed Turbomachinery, Hydrodynamic Journal Bearing.

1. INTRODUCTION

Floating-ring bearings (FRBs) play a critical role in high-speed turbomachinery by providing damping and stability. They consist of an outer ring that rotates between the journal and the bearing housing. This configuration forms dual lubrication films, reducing friction and heat generation, as shown in Figures 1. This class of journal bearings (JBs) is widely used in turbochargers, compressors, and gas turbines, where optimizing performance is essential to minimize energy losses and wear.

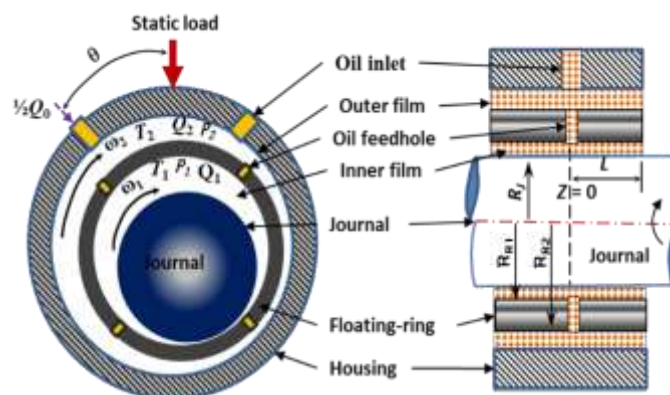


Figure 1: Description of FRBs and their 2 parallel films' arrangement

However, despite their advantages in damping and cooling, FRBs exhibit several rotordynamic defects that adversely impact their performance in high-speed turbo-machinery. These defects include low load-bearing capacity, hydrodynamic instability, non-linear dynamic behaviour, complex film dynamics, and potential for ring seizure [1,2]

Consequently, this study focuses on the semi-empirical characterization of the dynamic behaviour and the load-bearing capacity prediction of short FRBs for performance enhancement in high-speed turbomachinery. It adapts Reynolds equation-based models, classical rotordynamic equations and superposition principle of parallel films' dynamic parameters to achieve the research goal.

2. LITERATURE REVIEW

FRBs are a type of hydrodynamic bearing consisting of an outer ring that rotates between the journal and the housing. The presence of this floating ring introduces an additional lubrication film, leading to a reduction in friction and heat generation. Figure 2 shows a typical turbocharger rotor supported on a pair of FRBs.

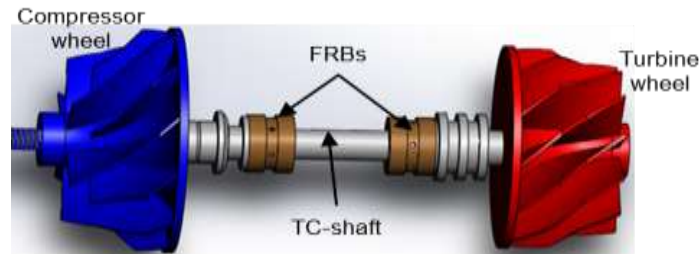


Figure 2: Floating-ring bearing supported turbocharger shaft

2.1 Analytical Models

Several theoretical models have been developed to describe the behaviour of FRBs, such as:

- Reynolds Equation-Based Models which predict FRB's dynamic characteristics and load-carrying capacity using the pressure distribution in the lubricant films [1];
- Thermo-Hydrodynamic (THD) Models that incorporate temperature effects on film viscosity variations and thermal expansion, which determine FRB's dynamic performance and load-bearing capacity [3,4]; and
- Dynamic Stability Models which predict rotordynamic performance of FRBs at critical speed, considering their damping characteristics, and whirl instability on rotor-bearing system [1, 5].

Factors Affecting FRBs Load-bearing Capacity and Stability

FRBs dynamic characteristics and stability performance are influenced by several factors. These factors should be carefully chosen and implemented to mitigate impacts of undesirable rotor instability, friction, and inadequate stiffness. They include: (i) Lubricant properties such as oil viscosity and supply pressure which significantly affect bearing instability, energy losses, and load capacity [1]; and (ii) Geometric considerations, such as clearance ratios, radius ratios, and film thickness [2, 6].

2.2 Investigating FRBs Load-bearing Capacity and Stability Performance

FRBs in automotive turbochargers are cost-effective and capable of handling extreme speeds. However, they often suffer from noise due to oil whirl-induced sub-synchronous vibrations, prompting the investigation into whether an elliptical clearance design could mitigate these issues. Figure 3 shows a substantial sub-synchronous instability of FRB [2]. By developing an efficient approximate solution to the Reynolds equation and conducting nonlinear run-up simulations, [7] found that an elliptical modification of the bearing improves steady-state performance and suppresses the self-excited vibrations.

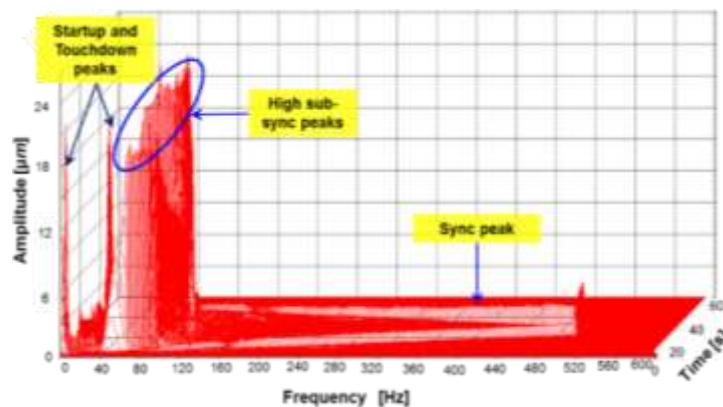


Figure 3: FRB signal waterfall indicating massive sub-sync peaks

To further explore these instabilities, [8] develops a nonlinear rotor model using fluid dynamic principles and numerical continuation to detect bifurcations and limit cycles. The research reveals that the bearing dynamic parameters critically influence rotor stability and necessitates safer, more rational design criteria. Some studies analyse how modifications in microgeometry, such as adding circumferential grooves in the outer film and tailored features in the inner film can mitigate these vibrations and reduce hydrodynamic power losses by over 10%, achieving approximately a 20% reduction in vibration compared to standard designs.

Consequently, [5] quantitatively investigate the rotordynamic instability in FRB-supported turbo-shafts by testing various feed-angles ($\Phi=0^\circ-60^\circ$) across 6.0–30 krpm instead of relying solely on conventional structural modifications. Their results demonstrate that larger injection angles reduce whirl frequency, orbit size, and sub-synchronous amplitudes by balancing pressure fields and enhancing damping, thereby significantly improving rotordynamic stability in high-performance turbo-systems.

In further research, [9] introduced an oil-injection swirl-control mechanism (OISCM) for FRBs, demonstrating that FRBs equipped with OISCM show significantly improved damping, lower whirl-frequency ratios, and reduced cross-coupled forces, particularly at higher OISCM angles and speeds above 22 krpm, as shown in Figure 4. Although OISCM may slightly decrease load capacity at lower speeds, they showed that increasing the oil-supply pressure effectively prevents inner-film starvation, making this approach more effective for mitigating rotordynamic instabilities than conventional FRBs.

Still on FRB geometry, [10] examine the noncircular three-lobe semi-floating ring-bearing structures (SFRBs) in marine turbochargers by using the half-step centre Finite Difference Method and Newton–Raphson iterative procedure. Their findings indicate that increasing oil supply pressure enhances the oil film thickness and film lubrication; and the load-bearing capacity is largest where film thickness is least and wall friction is most pronounced.

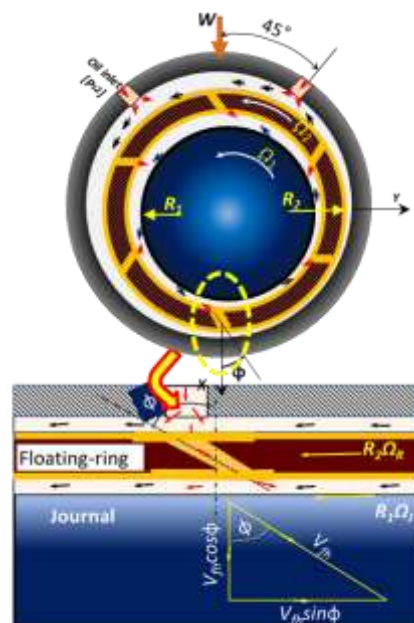


Figure 4: Schematic of FRB oil-injection swirl-control mechanism (OISCM) with the defining oil-injection angle (Φ)

They noted that stiffness and damping display notable nonlinear behaviour within the operational speed range. Furthermore, [11], finds that a multi-lobe floating ring design, validated through numerical run-up simulations and experimental measurements, significantly suppresses both synchronous and sub-synchronous vibrations, with only a slight increase in friction losses, making it a promising alternative for turbocharger applications.

Conversely, [12], study the dynamic behaviour of FRB-rotor systems using the transfer-matrix method and Runge–Kutta analysis to examine how the oil film clearance ratio impacts rotor stability and load capacity. They observe that an optimal clearance ratio of $\lambda = 0.01$ offers the best balance, providing substantial load capacity for the design and fault diagnosis of these high-speed machinery bearings. [13], evaluate a noncircular cylindrical floating ring bearing, using finite element analysis to solve the Navier–Stokes and continuity equations under laminar flow conditions. Their performance assessments based on parameters like film eccentricity, Sommerfeld number, stiffness and damping coefficients, and critical journal mass indicate that the noncircular design delivers significantly superior dynamic performance compared to the conventional plain bearing.

In furtherance, [14], employing the Navier–Stokes and continuity equations, investigates the impact of turbulence on a novel non-circular floating ring bearing, comprising a cylindrical journal and floating ring paired with a non-circular outer housing designed to improve stiffness. Its dynamic performance analysis over a range of outer film eccentricity ratios and Reynolds numbers up to 9000 confirms a satisfactory operation under turbulent conditions. Correspondingly, a genetic algorithm-based multi-objective optimization is applied by [15] to compute twelve design variables that minimize rotor eccentricity and power loss, significantly reducing computational demands compared to traditional methods while offering deeper insights into stability quality rather than just instability thresholds.

Again, research has shown that internal thread textures in semi-floating ring bearings significantly modify the dynamic characteristics of the oil film, such as maximum pressure, load-carrying capacity, stiffness, and damping, which in turn affect the vibration amplitude and operating life of turbocharger rotor systems. Using a hydrodynamic model and CFD analysis, [16] found that an optimal texture (with a 0.006 mm depth, 9 thread turns, and centered distribution) enhances oil film performance, offering valuable design guidelines to suppress rotor vibrations and improve bearing performance. [17], explore the effects of variations in the inner and outer oil film clearances of floating ring bearings on excessive and even nonlinear vibrations in high-speed turbochargers. They opine that using the right film clearance minimizes vibration amplitudes and prevents the onset of fractional frequency vibrations, thereby enhancing rotor stability and operational reliability.

Hybrid floating ring bearings at high speeds exhibit both laminar and turbulent flows in their inner and outer films. [18], using a unitized kinematic model based on the Routh–Hurwitz method show that mixed flow and thermal effects increase load capacity and friction moment while reducing threshold speed. Conversely, [19], investigate how oil inlet pressure and temperature affect the dynamic behaviour of turbocharger rotors supported by fully-floating ring bearings (FFRBs). Their analysis reveals that variations in oil conditions significantly influence rotor responses, including sub-synchronous vibrations and oil-induced instabilities.

3. METHODOLOGY

3.1 DYNAMIC COEFFICIENTS SUMMATION BY SUPERPOSITION

Figures 5 show the schematics of the arrangement of FRB dynamic parameters (i.e. inertia, stiffness, and damping). Let the governing equations of motions and forces on the bearing housing (H) and the floating ring (R) about their respective steady-state equilibrium positions ($SSEP$) be expressed as:

$$\left. \begin{aligned} M_H \ddot{\delta}_H + C_2 \dot{\delta}_{HR} + K_2 \delta_{HR} &= F_{ext}(t) \\ M_R \ddot{\delta}_R + C_1 \dot{\delta}_{RJ} + K_1 \delta_{RJ} &= C_2 \dot{\delta}_{HR} + K_2 \delta_{HR} \end{aligned} \right\} \quad (1)$$

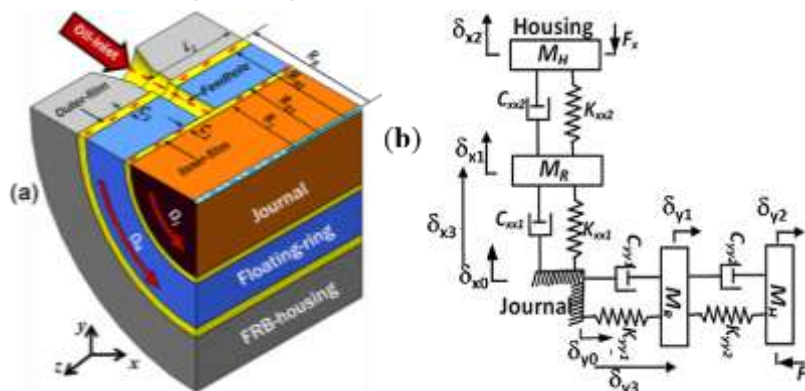


Fig. 5: Floating-ring bearing: (a) section view of assemblage, (b) free-body diagram

The Fourier solutions to the second order differential equations of the dynamic system are given in equations (2). Here, the symbols (M , K , C) are the 2-by-2 matrices of the inertia, stiffness and damping coefficients; while the notations (F_{ext} , δ) represent the 2-by-2 matrices of the external exciting forces and the corresponding displacements from $SSEP$, respectively. The single and double dots over any symbol(s) denote the first and the second order time derivatives, respectively. Subscripts (H , J , R) stand for the housing, journal, and the ring respectively; whereas (HJ , HR , RJ) represent their relative perturbation distances from each other. The notations (ω , t) represent the excitation frequency and time, respectively.

$$\left. \begin{aligned} -\omega^2 M_H \delta_H + (K_2 + i\omega C_2) \delta_{HR} &= F_{ext}(\omega) \\ -\omega^2 M_R \delta_R + (K_1 + i\omega C_1) \delta_{RJ} &= (K_2 + i\omega C_2) \delta_{HR} \end{aligned} \right\} \quad (2)$$

Assume that in Figure 5(b), the journal has no lateral displacements ($\Delta\delta_{Jx} = \Delta\delta_{Jy} = 0$); then $\delta_R = \delta_{RJ}$ and $\delta_H = \delta_{HJ}$. Thus, $\delta_H = (\delta_{HR} + \delta_{RJ})$, and equations (2) are rewritten as

$$\left. \begin{aligned} -\omega^2 M_H \delta_{RJ} + (K_2 - \omega^2 M_H + i\omega C_2) \delta_{HR} &= F_{ext}(\omega) \\ (K_1 - \omega^2 M_R + i\omega C_1) \delta_{RJ} &= (K_2 + i\omega C_2) \delta_{HR} \end{aligned} \right\} \quad (3)$$

Define the dynamic stiffness as $D_{(\omega)} = (K - \omega^2 M + i\omega C)$: then, equations (3) are expressed in terms of $D_{(\omega)}$ as

$$\left. \begin{aligned} -\omega^2 M_H \delta_{RJ} + D_{2(\omega)} \delta_{HR} &= F_{ext(\omega)} \\ D_{1(\omega)} \delta_{RJ} - (K_2 + i\omega C_2) \delta_{HR} &= 0 \end{aligned} \right\} \quad (4)$$

From equations (4), the mean displacements are derived and presented in equations (5). Note that equations (5) contain the relations representing the mean displacements for the inner and outer films, respectively. The 2 equations of (5) are subsequently superposed to yield the overall displacement as given in equation (6). Dividing through by $F_{ext(\omega)}$ produces the flexibility matrix $[H_{(\omega)}^{eq}]$ of equation (7). The inverse of the flexibility $[H_{(\omega)}^{eq}]$ generates the required FRB equivalent dynamic stiffness matrix $[D_{(\omega)}^{eq}]$ as presented in equation (8). It is pertinent to remark here that equations (7) and (8) are valid for FRBs as well as squeeze-film dampers.

$$\left. \begin{aligned} \delta_{RJ} &= [D_{1(\omega)}]^{-1} (K_2 + i\omega C_2) \delta_{HR} \\ \delta_{HR} &= \frac{F_{ext(\omega)}}{(D_{2(\omega)} - \omega^2 M_H [D_{1(\omega)}]^{-1} (K_2 + i\omega C_2))} \end{aligned} \right\} \quad (5)$$

$$\delta_{HJ} = \frac{\left[I + \frac{K_2 + i\omega C_2}{D_{1(\omega)}} \right]}{\left(D_{2(\omega)} - \frac{\omega^2 M_H (K_2 + i\omega C_2)}{D_{1(\omega)}} \right)} F_{ext(\omega)} \quad (6)$$

$$[H_{(\omega)}^{eq}] = \frac{[\delta_{HJ}]}{[F_{ext(\omega)}]} = \frac{\left[I + \frac{K_2 + i\omega C_2}{D_{1(\omega)}} \right]}{\left(D_{2(\omega)} - \frac{\omega^2 M_H (K_2 + i\omega C_2)}{D_{1(\omega)}} \right)} \quad (7)$$

$$\begin{bmatrix} D_{yy}^{eq} & D_{xy}^{eq} \\ D_{yx}^{eq} & D_{xx}^{eq} \end{bmatrix} = \frac{\begin{bmatrix} H_{yy}^{eq} & -H_{xy}^{eq} \\ -H_{yx}^{eq} & H_{xx}^{eq} \end{bmatrix}}{\begin{bmatrix} H_{xx}^{eq} H_{yy}^{eq} - H_{xy}^{eq} H_{yx}^{eq} \end{bmatrix}} \quad (8)$$

3.2 MODEL IMPLEMENTATION PROCEDURE

For π -film short bearing, are integrated numerically using Sommerfeld integrals to produce the non-dimensional force coefficients for the outer and inner films, respectively. The resulting 16 non-dimensional quantities are condensed by applying the superposition procedure using equations (7) and (8) to yield the required 8 equivalent force parameters for FRB. The ring speed ratio is computed from equation (9); while the Sommerfeld numbers are computed from equations (10) and (11). The effective film viscosities (μ_1, μ_2) as input variables are determined by thermal analysis for each journal-speed using Vogel's model. The quantities (Ω_R/Ω_J) , (μ_2/μ_1) and $(\varepsilon_2/\varepsilon_1)$ are required variables for estimating the force parameters. FRB dynamic force coefficients generated are used to compute the whirl frequency ratio (WFR). In rotor-bearing analysis, the WFR can be considered as a rotordynamic instability indicator.

$$\beta = \left(\frac{\lambda_\beta \left(\frac{\varepsilon_1}{\varepsilon_2} \right) \left(\frac{1 - \varepsilon_2^2}{1 - \varepsilon_1^2} \right)^2 \sqrt{\frac{16\varepsilon_1^2 + \pi^2(1 - \varepsilon_1^2)}{16\varepsilon_2^2 + \pi^2(1 - \varepsilon_2^2)}}}{\left(\frac{\mu_2}{\mu_1} \right) \left(\frac{P_1}{P_2} \right) \left(\frac{c_1}{c_2} \right)^2 \left(\frac{R_2}{R_1} \right)^3 + \left(\frac{\varepsilon_1}{\varepsilon_2} \right) \left(\frac{1 - \varepsilon_2^2}{1 - \varepsilon_1^2} \right)^2 \sqrt{\frac{16\varepsilon_1^2 + \pi^2(1 - \varepsilon_1^2)}{16\varepsilon_2^2 + \pi^2(1 - \varepsilon_2^2)}}} \right) \quad (9)$$

$$Sn_1 = \frac{\mu_1 (\Omega_J - \Omega_R) L D_1}{W} \left(\frac{R_1}{c_1} \right)^2 = \frac{(1 - \varepsilon_1^2)^2}{\pi \varepsilon_1 \sqrt{16\varepsilon_1^2 + \pi^2(1 - \varepsilon_1^2)}} \quad (10)$$

$$Sn_2 = \frac{\mu_2 \Omega_R L D_2}{W} \left(\frac{R_2}{c_2} \right)^2 = \frac{(1 - \varepsilon_2^2)^2}{\pi \varepsilon_2 \sqrt{16\varepsilon_2^2 + \pi^2(1 - \varepsilon_2^2)}} \quad (11)$$

4. RESULTS AND DISCUSSION

MODEL PREDICTIONS

4.1 Predictions for Eccentricities and Ring-to-Journal Speed Ratios

Figures 6 (a) to (d) display the plots of the floating-ring eccentricity (ε_2) and the speed ratio (N_R/N_J). The curves of Figure 14(a) indicate that when $P_2/P_1=1.0$, $c_2/c_1=1.0$ and $\lambda_e=1.0$, the ring's eccentricity is linearly proportional to the journal eccentricity. However, this does not hold for higher values of c_2/c_1 where the ring's eccentricity becomes a polynomial and slightly less sensitive to changes in ε_1 , especially for near centre-operations ($\varepsilon_1 \rightarrow 0$). In fact the minimum

ε_2 occurs at $\varepsilon_1=0$, and its value increases with the increase in c_2/c_1 , for fixed value of P_2/P_1 . Correctly estimating the values of ε_1 and ε_2 is a prerequisite for proper rotordynamic characterizing of FRB stability and load capacity.

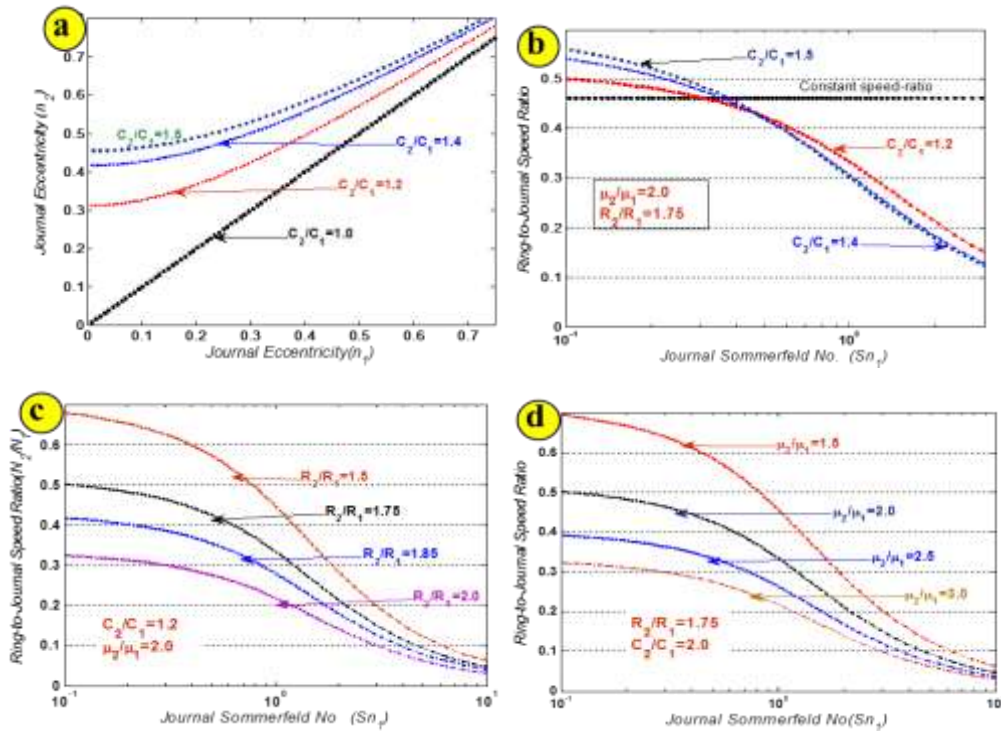


Figure 6: Dependencies of ring speed ratio on bearing dimensions and film viscosity

In Figure 6(b), the ring-to-journal speed-ratio (N_R/N_J) is weakly affected by the changes in c_2/c_1 ; but substantially by the inner-film Sommerfeld (Sn_1). The N_R/N_J drops sharply from 0.5 to 0.15 as the Sn_1 value is raised. High Sn_1 value implies an increased rotor-speed and/or a reduced bearing-load. Similarly, in Figures 6(c–d), the sensitivities of N_R/N_J to changes in R_2/R_1 and μ_2/μ_1 are enormous, particularly at low Sn_1 ; but become less significant at higher Sn_1 . The characteristic decrease of N_R/N_J due to a larger R_2/R_1 is attributed to the greater inertia against the accelerating torque: because the latter is proportional to inertia. Correspondingly, a higher value of μ_2/μ_1 implies a weaker inner-surface accelerating torque or a stronger outer-surface drag torque. Note that torque is directly proportional to the effective film-viscosity.

4.2 Prediction of Equivalent Force Coefficients of FRB

The steady state solutions for the eccentricities and ring-speed ratio are necessary input variables for the numerical evaluation of the FRB force parameters. Figures 7 and 8 present the non-dimensional force coefficients plotted against the inner-film Sommerfeld number and journal eccentricity, respectively. The direct stiffness coefficient (K_{xx}) is higher at low Sn_1 (or high ε_1); but begins to drop in magnitude until it attains a fairly steady value of 4.03 for $Sn_1 > 3.0$ (or $\varepsilon_1 < 0.1014$). On the other hand, the value of K_{yy} changes from 3.57 at low Sn_1 to 4.02 for $Sn_1 > 3.0$. The curves of K_{xx} and K_{yy} indicate that the direct stiffness terms do not vary monotonically with increasing Sn_1 . The cross-coupled stiffness terms (K_{xy} , K_{yx}) are significantly low compared to the direct terms, except for $Sn_1 > 10$ (or $\varepsilon_1 < 0.03$). This implies that a centre operating rotor could be unstable because of large K_{xy} and K_{yx} . Their curves, for $Sn_1 < 5.0$, are roughly the mirror images of each other about the x-axis.

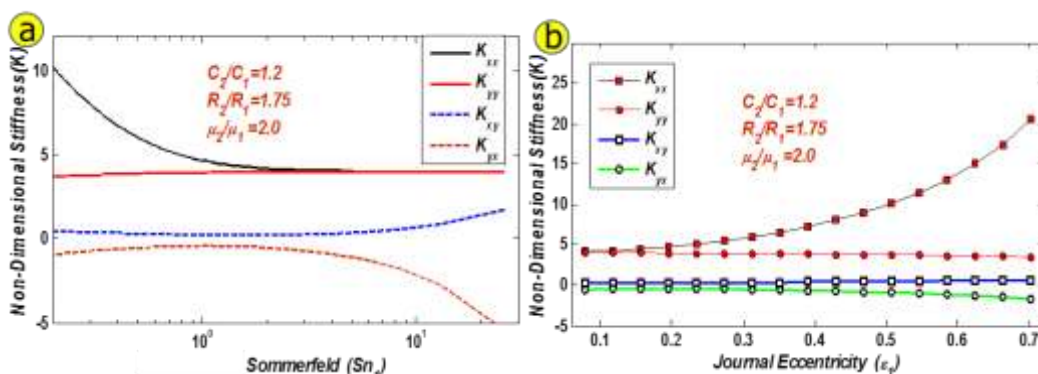


Figure 7: Predicted equivalent non-dimensional stiffness coefficients for FRB

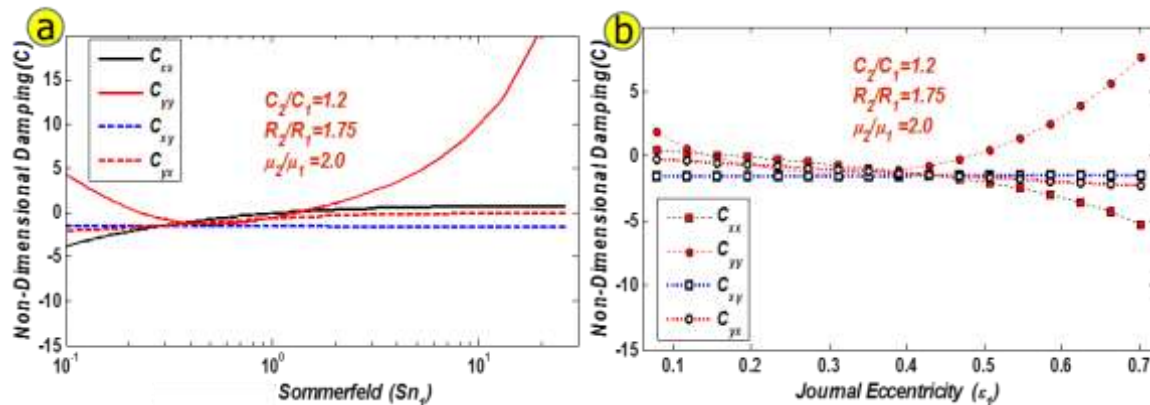


Figure 8: Predicted equivalent non-dimensional damping coefficients for FRB

On the other hand, the direct damping coefficients (C_{xx} , C_{yy}) are very sensitive to changes in Sn_1 and ϵ_1 , especially for extreme values. For instance, C_{yy} is very large in the range $4.3 < Sn_1 < 0.3$. Hence, their high magnitudes provide excellent damping to preclude possible total rotordynamic instability in light-load, high-speed turbomachinery. In addition, the cross-coupled damping terms (C_{xy} , C_{yx}) are generally very small and almost insensitive to changes in Sn_1 and ϵ_1 .

5. CONCLUSION

This study presents a semi-empirical characterization of floating-ring bearings (FRBs) to enhance the performance of high-speed turbomachinery. The findings reveal that the ring's eccentricity (ϵ_2) is strongly dependent on the journal eccentricity (ϵ_1), particularly when the ratio of ring-to-journal clearance (c_2/c_1) is low. However, as c_2/c_1 increases, the relationship becomes nonlinear, and the ring's sensitivity to ϵ_1 variations diminishes, especially in near-centre operations. Additionally, the ring-to-journal speed ratio (N_R/N_1) exhibits a sharp decline with increasing inner-film Sommerfeld number (Sn_1), signifying the influence of rotor speed and bearing load on FRB dynamics.

The force coefficients derived from the steady-state solutions underscore the complex interplay between stiffness and damping characteristics in FRBs. The direct stiffness coefficients (K_{xx} , K_{yy}) exhibit non-monotonic variations with Sn_1 , with K_{xx} stabilizing at higher values of Sn_1 while K_{yy} increases. Notably, cross-coupled stiffness terms (K_{xy} , K_{yx}) remain small except at extremely low eccentricities, suggesting potential instability at near-centre operations. The damping coefficients (C_{xx} , C_{yy}) play a crucial role in mitigating rotordynamic instability, particularly under high-speed, light-load conditions, where C_{yy} exhibits significant damping capability.

Therefore, this study provides critical insights into the dynamic behaviour of FRBs, emphasizing the importance of accurately estimating key parameters for improved stability and load-bearing performance in turbomachinery applications. The results serve as a valuable reference for optimizing FRB design, contributing to enhanced reliability and efficiency in high-speed rotating systems.

6. REFERENCES

- [1] L. San Andrés & J. Kerth, J. Thermal effects on the performance of floating ring bearings for turbochargers. Proceedings of the Institution of Mechanical Engineers, Part J: Journal of Engineering Tribology, 2004, 218, pp.437 - 450.
- [2] D. Tamunodukobipi, Y. Cho & Y. Lee, Feasibility Study of Instability Control of a Floating Ring Bearing for Turbocharger. Proceedings of Asian Congress on Gas Turbines, Seoul, Korea, ACGT2014-0156, 2014.
- [3] L. Huang, W.H. Tao, H. Liu, F. Gu & H. Zhang, Study on friction characteristics of journal bearings based on thermoelectric potential. Industrial Lubrication and Tribology, 2025.
- [4] R. Wang & L. Zhang, Effect of rotational speed on transient thermoelastohydrodynamic tribo-dynamic characteristics of journal bearings. Proceedings of the Institution of Mechanical Engineers, Part J: Journal of Engineering Tribology, 2024.
- [5] D. T.- I. Tamunodukobipi & Y.B. Lee, Rotordynamic Instability Control For Floating-Ring Bearing Supported Turbo-Shaft By Angled Oil-Injection Feedholes. International Journal of Engineering and Applied Sciences, 5, 2018.
- [6] J. Naranjo, C. Holt & L. S. Andrés, Dynamic Response of a Rotor Supported in a Floating Ring Bearing 1st International Conference in Rotordynamics of Machinery, ISCORMA1,2001.

- [7] C. Zhang, Y. Wang, R. Men, H. He & W. Chen, Dynamic behaviors of a high-speed turbocharger rotor on elliptical floating-ring bearings. *Proceedings of the Institution of Mechanical Engineers, Part J: Journal of Engineering Tribology*, 2019, Vol. 233, No.12, pp.1785-1799. <https://doi.org/10.1177/1350650119849743>.
- [8] A. Amamou, Nonlinear stability analysis and numerical continuation of bifurcations of a rotor supported by floating ring bearings. *Proceedings of the Institution of Mechanical Engineers, Part C: Journal of Mechanical Engineering Science*, 2022, Vol. 236, No.5, pp.2172-2184. <https://doi.org/10.1177/09544062211026340>.
- [9] D. T.- I. Tamunodukobipi, C.H. Kim & Y. –B. Lee, Dynamic Performance Characteristics of Floating-Ring Bearings With Varied Oil-Injection Swirl-Control Angles. *Journal of Dynamic Systems Measurement and Control-transactions of The Asme*, 2015, 137, 021002.
- [10] J. Dong, H. Wen, J. Zhu, J. Guo & C. Zong, Analysis of Thermo-Hydrodynamic Lubrication of Three-Lobe Semi- Floating Ring Bearing Considering Temperature–Viscosity Effect and Static Pressure Flow. *Lubricants*, 2024.
- [11] R. Eling, R.A.J.V. Ostayen & D.J. Rixen, *Multilobe Floating Ring Bearings for Automotive Turbochargers*, 2015.
- [12] L. Peng, H. Zheng & Z. Shi, Z. (2021). Performance of Relative Clearance Ratio of Floating Ring Bearing for Turbocharger-Rotor System Stability. *Machines*, 2021, No. 9, Vo.11, 285. <https://www.mdpi.com/2075-1702/9/11/285> .
- [13] S. Soni & D. Vakharia, Dynamic performance analysis of a noncircular cylindrical floating ring bearing. *Proceedings of the Institution of Mechanical Engineers, Part J: Journal of Engineering Tribology*, Vol.231, No.6, pp. 745-765. <https://doi.org/10.1177/1350650116677505>.
- [14] S. Soni, Turbulence effect on dynamic performance of non-circular floating ring bearing. *Proceedings of the Institution of Mechanical Engineers, Part J: Journal of Engineering Tribology*, 2021, Vol.235, No. 2, pp. 290-302. <https://doi.org/10.1177/1350650120916050> .
- [15] I. Polyzos, E. Dimou & A. Chasalevris, Coupling nonlinear dynamics and multi-objective optimization for periodic response and reduced power loss in turbochargers with floating ring bearings. *Nonlinear Dynamics*, 2024.
- [16] X. Zhong, J. Jiang, G. Bin, A. Chen & F. Yang, F. (2023). Vibration characteristics of turbocharger rotor system considering internal thread texture parameters of semi-floating ring bearing. *Proceedings of the Institution of Mechanical Engineers, Part J: Journal of Engineering Tribology*, 2023, Vol. 237, No.9, PP.1796-1808. <https://doi.org/10.1177/13506501231186845>.
- [17] L. Wang, G. Bin, X. Li & X. Zhang, Effects of floating ring bearing manufacturing tolerance clearances on the dynamic characteristics for turbocharger. *Chinese Journal of Mechanical Engineering*, 2015, 28, pp.530-540.
- [18] Y. Shuai, G. Hong, Z. Shao-lin & X. Bo-qian, Thermohydrodynamic Characteristics and Stability Analysis for a Journal Hybrid Floating Ring Bearing Within Laminar and Turbulent Mixed Flow Regime. *Journal of Tribology-transactions of The Asme*, 2021, 143.
- [19] I. –B. Lee & S.-K. Hong, Effects of Oil Inlet Pressure and Temperature on the Dynamic Behaviors of a Full-Floating Ring Bearing Supported Turbocharger Rotor, 2017.